JOURNAL OF WATER AND LAND DEVELOPMENT
e-ISSN 2083-4535

Polish Academy of Sciences (PAN) Institute of Technology and Life Sciences – National Research Institute (ITP – PIB)

JOURNAL OF WATER AND LAND DEVELOPMENT
DOI: 10.24425/jwld.2023.146601
2023, No. 58 (VII–IX): 89–98

Historical and projected land-use / land cover changes of the Welmel River Watershed, Genale Dawa Basin, Ethiopia

Solomon E. Ayalew[1)] ✉, Tewodros A. Nigussie[2)]

[1)] Ministry of Labor and Skills, Addis Ababa, Ethiopia

[2)] Hawassa University, Institute of Technology, Hawassa, Ethiopia

RECEIVED 28.06.2022 ACCEPTED 04.04.2023 AVAILABLE ONLINE 29.09.2023

Abstract: Human activities on land have grown significantly changing the entire landscape, while most of the changes have occurred in the tropics. The change has become a serious environmental concern at the local, regional and global scales. The intensity, speed, and degree of land use / land cover (LULC) changes are nowadays quicker compared to the past because of the development of society. Moreover, the rapid increase in population resulted in disturbing a large number of landscapes on the Earth. The main objective of this study was to detect historical (1990–2020) and predicted (2020–2050) LULC changes in the Welmel River Watershed, which is located in the Genale-Dawa Basin, South Eastern Ethiopia. The dataset of 1990, 2005, and 2020 was generated from Landsat 5, Landsat 7 and Landsat 8 respectively to determine the historical LULC map. The result of this study revealed that agriculture/settlement increased by 6.85 $km^2 \cdot y^{-1}$, while forestland declined by 9.16 $km^2 \cdot y^{-1}$ over the last 31 years between 1990 and 2020. In the coming 31 years (by 2050), if the existing trend of the LULC change continues, agriculture/settlement land is expected to increase from 290.64 km^2 in 2020 to 492.51 km^2 in 2050 at the rate of 6.73 $km^2 \cdot y^{-1}$, while forestland is expected to shrink from 690.48 km^2 in 2020 to 427.01 km^2 in 2050 by a rate of 8.78 $km^2 \cdot y^{-1}$.

Keywords: CA-Markov chain model, change detection, land use / land cover (LULC), Welmel Watershed

INTRODUCTION

The land use / land cover (LULC) change is one of the important concerns in many regions of the world (Belward and Skøien, 2015; Taelman *et al.*, 2016). The change has become a serious environmental concern at the local, regional and global scales (Mishra, Rai and Mohan, 2014; Zhan *et al.*, 2014; Kumar *et al.*, 2015). For thousands of years, human activities on land have grown significantly and changed the entire landscape, while most of the changes have occurred in the tropics (Shi *et al.*, 2012). The intensity, speed, and degree of LULC changes are nowadays quicker compared to the past because of the development of society. Moreover, the rapid increase in population disturbed a large number of landscapes on the Earth (Lambin and Meyfroidt, 2011). On the global scale, the urban land area increased by 346.4 thous. km^2 and grew by 1.3% from 1992 to 2016 (He *et al.*, 2019). Bearing in mind the existing trends in population density, by 2030, the urban land cover is expected to increase by 1.2 mln km^2 (Seto, Güneralp and Hutyra, 2012). These changes cause major environmental concerns today, including climate change, biodiversity loss and pollution of water, soils and air (Kumar *et al.*, 2015).

Many papers in the literature have shown that population growth is the main factor for the land use change in urban or rural areas and expansion of urban areas. Moreover, forest clearance for timber production and other purposes will likely accelerate over the coming decades to satisfy demands of the increasing population (Mengistu, 2009; Dereje, 2010; Geremew, 2013; Gebreslassie, 2014; Andualem and Gebremariam, 2015). Previous studies in different parts of Ethiopia have shown a rapid expansion of cultivated land at the expense of forestland in the country (Gebrehiwot, Taye and Bishop, 2010; Gebremicael *et al.*, 2013; Gashaw, Bantider and Mahari, 2014; Hassen and Assen, 2018). Evidence from several studies shows a high conversion of forests to agricultural and pasture land (Mango *et al.*, 2011; Yeshaneh *et al.*, 2013). According to FAO (2010) in East Africa,

many hectares of original forest were lost in the last 20 years, and the remaining forest is fragmented and endangered.

On the other hand, recent data on the forest resources in Ethiopia reported by FAO (2010) places Ethiopia among countries with a forest cover of 10–30%. According to this report, the Ethiopia's forest cover is 12.2 mln ha (11%). It further indicated that the forest cover showed a decline from a 15.11 mln ha in 1990 to 12.2 mln ha in 2010, during which 2.65% of the forest cover was devastated. The Ethiopian highlands, covering almost half of the country, are affected by severe LULC and land degradation problems (Haregeweyn *et al.*, 2015; Gashaw *et al.*, 2018). Because of the high increase in population, a rapid expansion of cultivable lands has significantly reduced land with natural vegetation (Gebremicael *et al.* 2013; Ariti, Vliet van and Verburg, 2015; Haregeweyn *et al.*, 2017). Monitoring and mitigating the negative consequences of LULC while sustaining the production of essential resources have therefore become a major priority for researchers and policymakers around the world (Kumar *et al.*, 2015).

Determining and modelling historical patterns of change help to understand better the processes of change that help improve land management practices (Behailu, 2010; Aithal *et al.*, 2013). There are many LULC change models with their strong sides and limitation though there is no clearly prioritised approach to model LULC changes (Gidey *et al.*, 2017). However, the Markov Chain and Cellular Automata Analysis (CA-Markov) model, a hybrid of the cellular automata and Markov models, is the most commonly used spatially explicit model in recent literature because of its consideration to spatial and temporal components of the LULC dynamic (Behera *et al.*, 2012; Gashaw *et al.*, 2017). It is a discrete-time stochastic model, describing the probabilistic movement from one state (LULC type) to another state (LULC type) (Gidey *et al.*, 2017). The 'Cellular Automata' and 'Markov Chain' models are considered to be advantageous for modelling land-use changes (Amini Parsa, Yavari and Nejadi, 2016; Mishra and Rai, 2016).

In the Bale Mountain Eco-Region, Ethiopia, the Welmel River Watershed, which is one of the suppliers of the Genale Dawa Basin, is currently characterised by severe land degradation. The natural vegetation has been replaced by cultivable and grazing lands (Hailemariam, Soromessa and Teketay, 2016; Mezgebu and Workineh, 2017; Ayele, Hayicho and Alemu, 2019). Currently, the watershed area in the basin is under increasing threat from forest degradation, overgrazing by livestock, expansion of the agricultural area, disturbance of water systems, unsustainable fuel wood and timber extraction, fire and rapid immigration with unplanned and unrestricted settlement (SOS Sahel Ethiopia, 2010; Hailemariam, Soromessa and Teketay, 2016). Due to rapid urbanisation, new development is very often located on hazard-prone sites, including river banks and flood plains, which increases the exposure and vulnerability to climate and disaster risk (UNDP, 2016).

Hence, there is an urgent need to limit the current consumption patterns of spatial resources and for rational use of areas that are subject to urbanisation (Kazak, 2018). Analyzing and understanding these LULC changes is important for policymaking, planning, and implementation of natural resource management. Therefore, assessing historical and upcoming LULC changes can be essential to environmental management and future planning. Based on this, the main objective of this study was to assess three historical periods of 1990, 2005, and 2020, and predict possible land use / land cover (LULC) changes by 2050.

MATERIALS AND METHODS

STUDY AREA

The Welmel River is located in the South-Eastern part of Ethiopia in the Genale Dawa Basin (Fig. 1). The River originates from the northeastern of the Bale Mountains and drains into the Genale Dawa River. Geographically, the Welmel River Watershed is located between 6°8'0" N and 6°50'0" N, and 39°27'0" E and 39° 55'0" E latitudes and longitudes, respectively with an elevation ranging from 1035 to 4290 m a.s.l. The watershed covers a total land area of 1,461.54 km^2 in the Genale Dawa River basin.

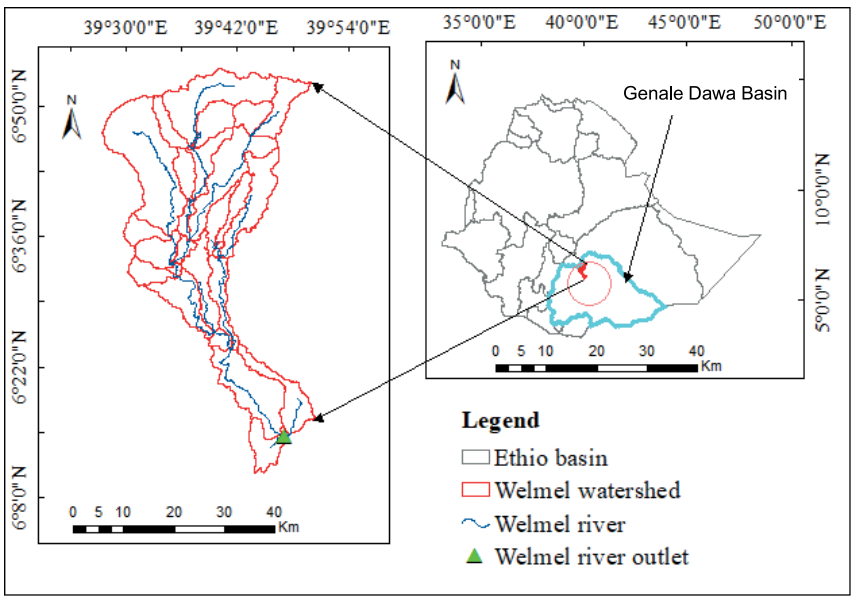

Fig. 1. Map of the study area; source: own elaboration

The total population residing in this part of the catchment is around 6719 out of which 3369 are males and 3350 are females. The most important economic activities of the study area include large agropastoral livelihoods, though in recent years sedentary farming appears to be the favoured trend due to climatic and socio-economic factors (MoWR, 2007). The rural community household income (livelihoods) primarily comes from crop production and animal rearing. However, small proportions of additional income for the community come from timber and non-timber forest products, non-farm labour, farm land lease, and petty trade.

LAND USE / LAND COVER

The LULC of 2020 Landsat satellite imageries was downloaded from the free USGS Glovis website (http://earthexplorer.usgs.gov), classified by the maximum likelihood supervised classification algorithm using ERDAS Imagine 2014 and the layout was prepared on ArcGIS10.4. The LULC of 2020 map (Fig. 2) was part of the result referring to the historical LULC change. As shown in Figure 2, the major land use / land cover in the study area includes forestland, rangeland, scrubland/bushland, woodland, agricultural land and scattered rural settlements. This includes the common natural vegetation of the LULC category that is found in the area, i.e. coniferous forest, dominated by *Juniperus procera* (Gatira) and *Afrocarpus gracilior* (Birbirsa), and Juniperus forest associated with *Hagenia abyssinica* and trees of *Olea europaea*. The middle catchment area is well-covered with forest vegetation. At lower altitudes, the dominant vegetation is woodland. Agriculture (agriculture/settlement) prevails in the lower area. Types of crops grown in the area include: maize, teff, sorghum and sesame among annual crops and coffee and fruits among perennial crops.

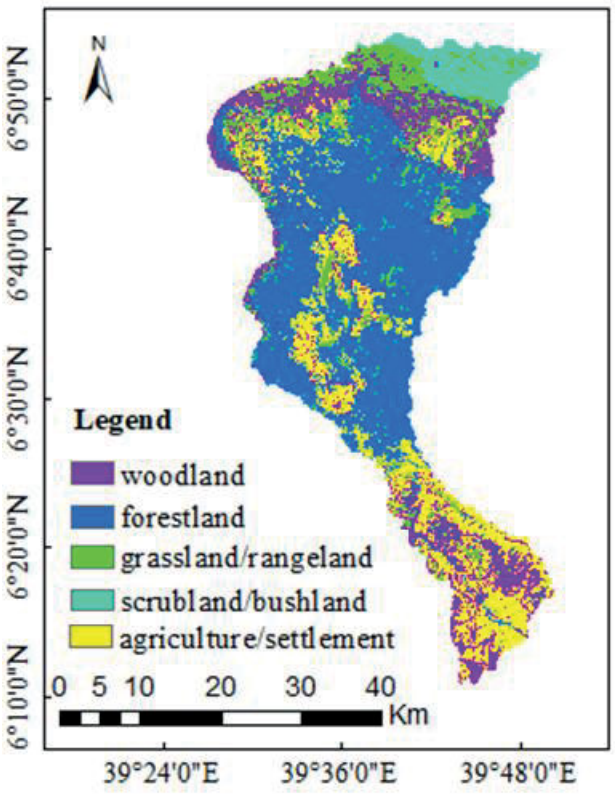

Fig. 2. Current (2020) land use / land cover map of Welmel Watershed; source: own elaboration

STUDY METHODS

Historical land use / land cover classification

The Landsat satellite imageries of the study area for 1990, 2005 and 2020 were downloaded from free USGS Glovis website (http://earthexplorer.usgs.gov) and used for the detection of historical and prediction of the future land use / land cover change in the Welmel River Watershed. These yearly images were selected primarily because a resettlement program was implemented there by the Derge Government in 1985/1986. Additionally, a participatory forest management was implemented by Farm Africa and SOS Sahel starting from 2005/2006 (Mezgebu and Workineh, 2017). The second reason was the availability of discharge data at Melka Amana gauged station starting from 1990. The datasets of 1990, 2005 and 2020 (Tab. 1) were generated from Landsat 5, Landsat 7 and Landsat 8 respectively. All images used in this study had 30 m spatial resolution. The time of extraction of the Landsat satellite imagery was selected to condense the consequence of cloud cover and periodic differences in the classification outcome.

Table 1. Details of landsat satellite imagery data

Year	Landsat	Sensor ID	Path/row	Acquisitions date
1990	Landsat 5	TM	167/55	01/25/1990
		TM	167/56	01/25/1990
		TM	168/55	02/17/1990
2005	Landsat 7	ETM+	167/55	01/10/2005
		ETM+	167/56	01/10/2005
		ETM+	168/55	01/01/2005
2020	Landsat 8	OLI/TIRS	167/55	01/09/2020
		OLI/TIRS	167/56	01/25/2020
		OLI/TIRS	168/55	01/16/2020

Explanations: TM = Thematic Mapper, ETM+ = Enhanced Thematic Mapper Plus, OLI/TIRS = Operational Land Imager / Thermal Infrared Sensor.
Source: own elaboration.

The study included satellite image pre-processing, layer stacking, mosaicking and image sub-setting for 1990, 2005 and 2020 using ERDAS Imagine 2014 before image classification to create multi-band composite images since the study area lies on three scenes. In this study for the LULC change detection, an unsupervised classification was first employed to get information about the overall LULC classes of the study area. Then supervised classification was employed to categorise images using ground truths (training areas) which were defined based on the results of unsupervised classification and ancillary data (Google Earth) (Saah *et al.*, 2019). ERDAS Imagine 2014 was employed for the classification of LULC and ArcGIS10.4 for mapping purposes.

Prediction of future LULC changes

This study employed a cellular automata model (CA-Markov) with a combination of the Markov Chain model to forecast future 2035 and 2050 LULC changes in the Welmel River watershed.

These two years were selected based on the interval of historical LULC changes at 15-year intervals. CA-Markov model requires three types of data inputs to project a LULC change (Hyandye and Martz, 2017). These are the basic temporal LULC image, Markov transition areas file, and transition suitability images generated using the Markov Chain model. The basic temporal LULC was prepared after the satellite image classification. The Markov transition area files were produced by running a Markov model before performing a CA-Markov module during the implementation of the Markovian LULC change modelling. The CA model generally uses the following formula (Subedi and Thapa, 2013; Camara *et al.*, 2020).

$$S(t, t+1) = f(S(t), N) \tag{1}$$

where: $S(t + 1)$ = system status at the time of $(t, t + 1)$, functioned by the state probability of any time (N).

The Markov chain model is often used in LULC monitoring, ecological modelling, simulation changes, trends of the LULC, and to predict the extent of land use change and stability of future land development in the area concerned (Subedi and Thapa, 2013; Amini Parsa, Yavari and Nejadi, 2016). The Markov chain model examines LULC changes in time to predict the future change (Kumar, Radhakrishnan and Mathew, 2014). Equation (1) explains the calculation for the prediction of LULC changes (Markov chain model):

$$S(t, t+1) = P_{ij} S(t) \tag{2}$$

where: $S(t)$ = system status at the time of t, $S(t + 1)$ is the system status at the time of $(t + 1)$, P_{ij} = transition probability matrix in a state which is calculated as follows (Sang *et al.*, 2011; Kumar, Radhakrishnan and Mathew, 2014):

$$P_{ij} = \begin{bmatrix} P_{1,1} & P_{1,2} & \dots & P_{1,N} \\ P_{2,1} & P_{2,2} & \dots & P_{2,N} \\ \dots & \dots & \dots & \dots \\ P_{N,1} & P_{N,2} & \dots & P_{N,N} \end{bmatrix} \tag{3}$$

$$0 \leq P_{ij} \leq 1 \tag{4}$$

where: P = transition probability; P_{ij} = probability of transforming from present state i to another state j in succeeding time; P_N = state probability of any time; the high transition has a probability near 1 and the low transition will have a probability near 0 (Kumar, Radhakrishnan and Mathew, 2014).

Model validation

In this study, the LULC maps of 1990 and 2005 were used as inputs for model verification. Based on this, Markov Chain outputs are used to prepare transition areas matrix, transition suitability image collection matrix, and a set of conditional probability images for the validation of the model. The transitional probability matrix comprises probability of each LULC class changes down to every single other class and the transitional area matrix comprises the number of pixels that are expected to be transformed from one LULC class to another over a period of time. On the other hand, the output conditional probability images denotes the probability of individual LULC classes in each pixel over time. The 1990 and 2005 historical LULC maps were used to produce a simulated LULC map for 2020 for the validation of the model by comparing it with the actual LULC map of 2020 through the *KIA* (Kappa index of agreement) approach (Hua, 2017). In this case, the LULC map of 2005 was used as the base map to predict the 2020 LULC map.

For validation, the level of agreement for Kappa indices is as follows: Kappa ≤ 0.5 indicates rare agreement, 0.5 ≤ Kappa ≤ 0.75 indicates a medium level of agreement, 0.75 ≤ Kappa < 1.0 indicates a high level of agreement, and Kappa = 1.0 denotes perfect agreement (Keshtkar and Voigt, 2016; Singh *et al.*, 2018). The result is usually between 0 and 1. Kappa for no information (K_{no}) indicates the proportion classified correctly relative to the expected proportion classified correctly by simulation, with no ability to specify the quantity of location accurately and Kappa for location (K_{location}) measures the validation between classified maps and the simulated map based on a specified location, while Kappa for standard (K_{standard}) indicates the proportion assigned correctly versus the proportion that is correct by chance (Araya and Cabral, 2010). According to Omar *et al.* (2014), the equations express statistics for Kappa variations are:

$$K_{\text{no}} = \frac{M(m)N(n)}{P(p) - N(n)} \tag{5}$$

$$K_{\text{location}} = \frac{M(m)N(m)}{P(m) - N(m)} \tag{6}$$

$$K_{\text{standard}} = \frac{M(m)N(n)}{P(p) - N(m)} \tag{7}$$

where: $N(n)$ = no information, $M(m)$ = medium grid cell-level information, $P(p)$ = perfect grid cell-level information across the landscape.

After successful validation of the model, the techniques were repeated using transition probabilities for 2005 and 2020 maps to predict LULC maps of 2035 and 2050, using the LULC map of 2020 as a base map. Then, changes in LULC were evaluated using 1990, 2005 and 2020 for historical LULC with a baseline map of 1990. Similarly, the predicted LULC change was evaluated using 2035 and 2050 with the baseline LULC map of 2020.

Accuracy and change analysis

The accuracy assessment for 1990 and 2005 under this study was performed using Google Earth by integrating it with ERDAS Imagine 2014 and collecting a total of 90 and 100 points from Google Earth respectively. In the case of 2020 classified image of accuracy assessment was performed by collecting a total of 115 Ground Control Points using GPS. The error matrix accuracy assessment of statistical analysis was used to determine the effectiveness of pixels grouped into the correct feature class. The columns of the matrix depict the number of pixels per class for reference data, and the rows show the number of pixels per class for the classified image. From this error matrix, overall accuracy, user's and producer's accuracy were determined. After the LULC maps were classified, a change detection analysis was conducted to examine the extent of LULC changes that occurred during the study period and to make useful decisions. To determine the amount of change among periods, Berihun *et al.* (2019) stated

that percent changes of individual LULC categories were calculated as follows:

$$\text{Percent change } (\%) = \frac{A_2 - A_1}{A_1} 100 \quad (8)$$

where: A_1 = area in year 1, A_2 = area in year 2 of a LULC class (km^2). While the rate of change of the classified LULC maps (Gashaw *et al.*, 2017; Berihun *et al.*, 2019) is estimated as follows:

$$\text{Change rate} = \frac{A - B}{Z} \quad (9)$$

where: change rate = rate of change ($km^2 \cdot y^{-1}$), A = the area of LULC (km^2) at time t –2, B = area of LULC (km^2) at time t – 1, Z = time interval between A and B (years).

RESULTS

This study investigated land use / land cover changes over three time periods: 1990–2005, 2005–2020 and 2020–2050. The LULC change data presented for this study is within the average rate of change because it is not known if the changes are linear as the development of land-use change is leap development. The accuracy assessment of the classified historical LULC attained in the analysis of the error matrix indicates an overall accuracy of 85.22% and 83.48% with a kappa statistic of 81.86% and 78.34% for the LULC map of 1990 and 2005 (Tab. S1) respectively. The overall accuracies of 88.69% and kappa statistics of 85.1% for the LULC maps of 2020 were attained.

The major types of LULC for the Welmel watershed are forestland, agriculture/settlement, woodland, scrubland/bushland and grassland/rangeland. Rivers, streams and springs were not included in the classification. This is due to the image resolution problem (30 m) and the very low likelihood of distinguishing springs and rivers from riverine vegetation (Mezgebu and Workineh, 2017). Similarly, it was difficult to distinguish settlements especially rural settlements from agricultural land on a 30 m spatial resolution image and in most cases, the two are spatially integrated. Therefore, settlements were grouped under agricultural land covers. This classification agrees with Gashaw, Bantider and Mahari (2014) and Mezgebu and Workineh (2017) who grouped agriculture and settlement under one class for the same reason listed above.

During the detection of historical LULC change, the classified LULC for the Welmel Watershed from 1990 to 2020 (Fig. 3) showed a significant LULC change (Tab. 2). In 1990–2020, woodland, forestland and grassland/rangeland areas were converted into agriculture/settlement in the downstream, middle and upper streams of the watershed.

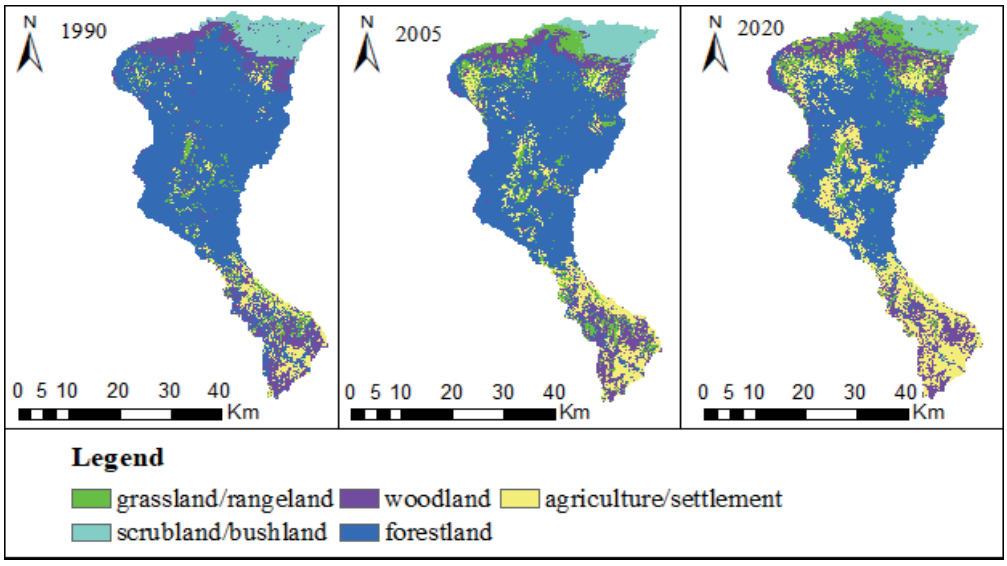

Fig. 3. Land use / land cover maps of 1990, 2005, and 2020 of the study areas; source: own study

Table 2. Historical land use / land cover (LULC) and their average rate of change from 1990–2020 in the study area

Land use / land cover class	Amount of area in km^2 under each year			Rate of change in $km^2 \cdot y^{-1}$		
	1990	2005	2020	1990–2005	2005–2020	1990–2020
Grassland/rangeland	73.84	156.96	152.41	+5.54	–0.30	+2.62
Scrubland/bushland	113.49	92.28	82.75	–1.41	–0.64	–1.02
Woodland	223.99	205.36	245.27	–1.24	+2.66	+0.71
Forestland	965.13	848.86	690.48	–7.75	–10.56	–9.16
Agriculture/settlement	85.09	158.07	290.64	+4.87	+8.84	+6.85

Source: own study.

Between 2005 and 2020, agriculture/settlement and woodland increased by 8.84 $km^2 \cdot y^{-1}$ and 2.66 $km^2 \cdot y^{-1}$ respectively. The historical and predicted LULC conversions from one LULC category to another between 1990 and 2020 were presented in (Tab. S2). The diagonals in the matrix from the table indicate unchanged areas, while the off-diagonals are the changes from one class to another. In 1990–2020, 124.17 km^2 of forestland was converted to agriculture/settlement, 65.65 km^2 to grassland/rangeland, 110.27 km^2 to woodland and 0.08 km^2 to scrubland/bushland. Moreover, 3.16, 4.50 and 16.14 km^2 of agriculture/settlement changed to forestland, grassland/rangeland and woodland respectively.

During the study period, 0.87, 2.14, 24.25 and 9.61 km^2 of scrubland/bushland changed into agriculture/settlement, forestland, grassland/rangeland and woodland respectively. Similarly, 69.03, 12.17, 45.40 and 3.20 km^2 of woodland changed into agriculture/settlement, forestland, grassland/rangeland and scrubland/bushland respectively. Moreover, 28.00, 2.06, 0.16 and 10.24 km^2 of grassland/rangeland has changed to agriculture/settlement, forestland, scrubland/bushland and woodland orderly.

During the determination of the predicted LULC change, the CA-Markov model validation result indicated a high level of agreement between observed and projected 2020 LULC maps (Fig. 4). Based on this, the result of various Kappa indices (*KIA* or $K_{standard}$) and respective statistics were computed. The Kappa statistics of $K_{standard}$ = 0.81, K_{no} = 0.86, and $K_{location}$ = 0.86 were obtained in the validation process which indicated a high level of agreement between the projected and observed LULC maps for 2020. This indicated that the model forecast was reliable. The result of the LULC change indicated that from 2020 to 2035 grassland/rangeland would increase (Tab. 3).

In the Welmel watershed, woodland will increase at an annual rate of 4.11 $km^2 \cdot y^{-1}$ as a result of the conversion of forest to woodland, while forest and scrubland/bushland area will decrease at 12.97 and 1.37 $km^2 \cdot y^{-1}$ respectively. Agriculture/settlement will increase from 290.64 to 412.23 km^2 at a rate of change of 8.11 $km^2 \cdot y^{-1}$ between 2020 and 2035 (Tab. 3).

In the Welmel watershed, from 2035 to 2050, agriculture/settlement is expected to increase at a rate of 5.35 $km^2 \cdot y^{-1}$, while forestland will decrease at a rate of 4.59 $km^2 \cdot y^{-1}$. On the other hand, scrubland/bushland and grassland/rangeland will decrease at a rate of 0.45 and 0.36 $km^2 \cdot y^{-1}$ respectively. On the contrary, woodland will increase at a rate of 0.05 $km^2 \cdot y^{-1}$.

Table S2 indicates the conversion matrixes result of the predicted LULC map from 2020 to 2050 with the baseline LULC map of 2020. It indicated that 113.13 km^2 of forestland would convert to agriculture/settlement, 44.19 km^2 to grassland/rangeland, and 96.74 km^2 to woodland. On the other hand, 41.60 km^2

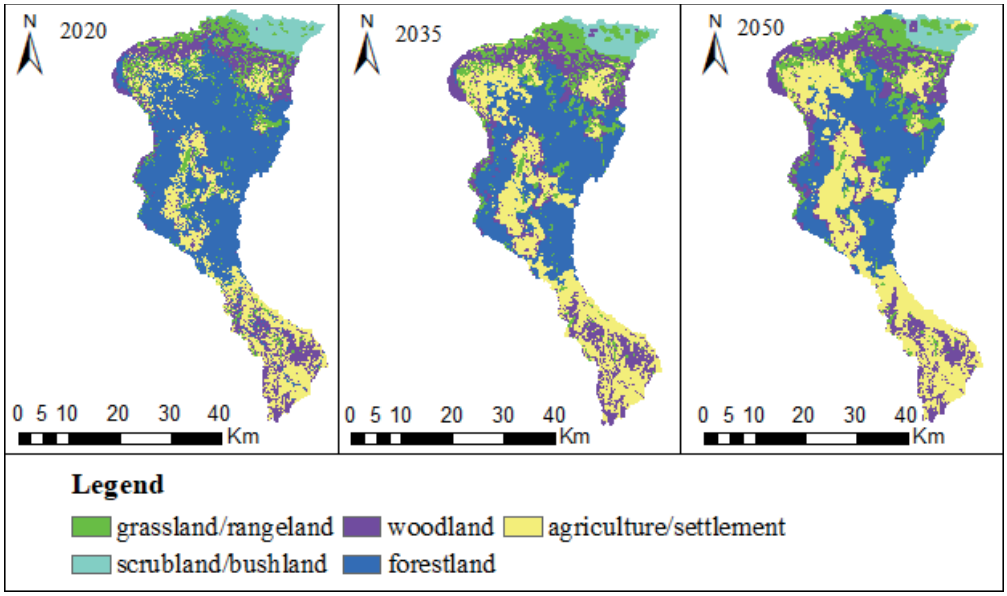

Fig. 4. Predicted land use / land cover maps of 2035 and 2050 with the baseline map of 2020; source: own study

Table 3. Predicted land use / land cover (LULC) and their rate of change in the study area in 2020–2050

Land-use / land cover class	Amount of area in km^2 under each year			Rate of change ($km^2 \cdot y^{-1}$)		
	2020	2035	2050	2020–2035	2035–2050	2020–2050
Grassland/rangeland	152.41	184.26	178.86	+2.12	–0.36	+0.88
Scrubland/bushland	82.75	62.22	55.48	–1.37	–0.45	–0.91
Woodland	245.27	306.95	307.68	+4.11	+0.05	+2.08
Forestland	690.48	495.88	427.01	–12.97	–4.59	–8.78
Agriculture/settlement	290.64	412.23	492.51	+8.11	+5.35	+6.73

Source: own study.

of woodland, 4.25 km^2 of scrubland/bushland, and 33.32 km^2 of grassland/rangeland are expected to convert to agriculture/settlement.

DISCUSSION

The accuracy assessment of the classified historical LULC result obtained from the analysis of the error matrixes shows that it is acceptable for further analysis. In support of the accuracy assessment, Mango (2010) stated that an overall accuracy between 60% and 90% is acceptable, and Matlhodi *et al.* (2019) quantified that a Kappa statistic of 0.7 fulfills the minimum established criteria for further analysis. Thus, in the study area of the Welmel watershed, the overall accuracy and kappa statistic result of the LULC category indicate an acceptable limit. The result of the historical LULC change under this study was almost consistent with the study by Aredo, Hatiye and Pingale (2021) in the Shaya catchment, the Genale-Dawa River basin, which reported that rangeland increased between 1987 and 2000 while decreasing between 2000 and 2015. Mezgebu and Workineh (2017) in Goba, Harena Buluk and Delo Mena Woreda, reported an increase in agriculture/settlement throughout the study period from 1986 to 2016, while forestland decreased. Moreover, the authors specifically reported the expansion in grassland/rangeland from 1986 to 2016 and scrubland/bushland decline between 1996 and 2006. The results of the historical LULC change under this study from 1990 to 2020 indicated that forestland declined, while agriculture/settlement increased. The LULC showed a significant change especially in forestland and agriculture/settlement from 2005 to 2020 compared with that of the 1990–2005 LULC map. Agriculture/settlement land showed a consistent increase, while scrubland/bushland and forestland showed a decreasing tendency over the study period from 1990 to 2020. Agriculture/settlement and grassland/rangeland increased between 1990 and 2005 at a rate of 4.87 and 5.54 $km^2 \cdot y^{-1}$ respectively. The increase in woodland between 2005 and 2020 occurred because of the conversion of forestland into woodland, and as woodland was converted into agriculture/settlement in other cases the reduced woodland area might be compensated by the conversion of forestland into woodland in the study area. However, forestland, scrubland/bushland, and grassland/rangeland decreased at a rate of 10.56, 0.64, and 0.30 $km^2 \cdot y^{-1}$ respectively.

This study indicated that the most significant change occurred in forestland, agriculture/settlement and grassland/rangeland in the Welmel watershed. The highest decrease in forests and increase in agriculture/settlement areas was observed between 2005 and 2020 (Tab. 2). This is might be due to the highest increasing demand for agriculture/settlement areas. Over the last 31 years, agriculture/settlement areas expanded, while forestland areas showed a sensational reduction followed by scrubland/bushland. Overall, from 1990 to 2020, forestland declined, while agriculture/settlement increased. In support of this result, Aredo, Hatiye and Pingale (2021) in the Genale-Dawa Basin Shaya catchment noted that woodland increased from 2000 to 2015. Moreover, specifically, the author reported that settlement and agricultural land showed increasing trends throughout the study period between 1987 and 2015. Aragaw, Goel and Mishra (2021) observed in the Gidabo River basin in Ethiopia that woodland increased from 2000 to 2018. Ayele, Hayicho and Alemu (2019) noted that the coverage in agriculture and settlement showed an increasing trend while bushland and forestland declined in Delo Mena district from 2000 to 2015. The conversion of 110.27 km^2 of forestland to woodland between 1990 and 2020 in the study areas might be the result of the incremental increase in woodland between 2005 and 2020. In agreement with this result, Mezgebu and Workineh (2017) in Goba, Harena Buluk and Delo Mena Woreda stated that forestland was mainly converted to agriculture/settlement and woodland between 1986 and 2016. Studies conducted in various parts of the country also reported conversions of one category to another. For instance, research was conducted in the Andassa watershed, Blue Nile Basin from 1985 to 2015 (Gashaw *et al.*, 2017) and Upper Gilgel Abbay catchment of Blue Nile basin (Rientjes *et al.*, 2011).

In the period between 2020 and 2035, grassland/rangeland is expected to increase. This increase might be due to fallowing of agricultural land and the conversion of scrubland/rangeland and woodland into grassland/rangeland class in the study area. In support of this result, Dibaba, Demissie and Miegel (2020) stated that the increase in rangeland in the Finchaa catchment from 2017 to 2036 might be associated with fallowing of agricultural land. The predicted LULC between 2020 and 2035 shows that agriculture/settlement, woodland and grassland/rangeland classes will increase due to the conversion of scrubland/bushland and forestlands into these LULC classes. This result is in line with the study conducted by Mezgebu and Workineh (2017), in Goba, Harena Buluk and Delo Mena Woreda by 2026. Another study by Ayele, Hayicho and Alemu (2019) in the Delo Mena district also suggests that the forest area will decline between 2010 and 2030, and woodland, farmland and settlement areas will increase by 2030. The expansion rate for the agriculture/settlement areas from 2020 to 2035 in the Welmel Watershed is higher compared to 2035 to 2050, which might be due to the limited areas available for agriculture/settlement expansion in the future. Tadese, Soromessa and Bekele (2021) in Gambella, Southwestern Ethiopia, reported that the area of forestland and grassland would show a decreasing trend, while farmland and settlement will continue to increase between 2032 and 2047. Another study conducted in Nashe Watershed, the Blue Nile River Basin by Leta, Demissie and Tränckner (2021) reported that forestland would decrease between 2019 and 2050 at a high increasing rate for urban areas and agricultural land. The reduction of forest area from 2020 to 2035 is higher compared to 2035 to 2050 in the study area of the Welmel watershed. This might be due to the diminishing coverage of forest areas between 2035 and 2050. The result of this study shows that in the future between 2020 and 2050, agriculture/settlement will increase at a rate of 6.73 $km^2 \cdot y^{-1}$, while forestland will decrease at a rate of 8.78 $km^2 \cdot y^{-1}$.

In the study area of the Welmel Watershed, 13.26 km^2 of woodland, 16.13 km^2 of scrubland/bushland, 44.19 km^2 of forestland, and 1.22 km^2 of agriculture/settlement land are expected to convert to grassland/rangeland between 2020 and 2050. This might be the reason for the incremental growth in grassland/rangeland from 2020 to 2050. When we compare the gain and loss of grassland/rangeland, it is expected to gain 74.8 km^2 and lose 41.79 km^2 of the area with a net gain of 33.01 km^2 in the future. On the contrary, the total area of 26.02 km^2 of scrubland/bushland is expected to change to other LULC types in the future. When comparing the gain and loss in woodland, it will gain 114.6 km^2 and lose 54.89 km^2, which results

in a net gain of 59.71 km^2. In a similar vein, Buraka, Elias and Lelago (2022) noted that bushland, grassland and agriculture/rural settlement would be converted to forestland. Conversely, forestland would be converted to bushland, agriculture/rural settlement, built-up area, bare land and water body respectively in Coka Watershed Southern Ethiopia, from 2018 to 2060. Moreover, Yohannes *et al.* (2020) stated that the conversion of LULC from one type to another would occur in Beressa Watershed, Blue Nile basin Ethiopian highlands, in 2017–2047.

CONCLUSIONS

This study indicated that the area of agricultural/settlement land increased by more than threefold between 1990 and 2020. A similar pattern can be seen between 2020 and 2050 during the projected periods. However, forestland decreased during both the historical and projected periods. In particular, it can be concluded that the expansion of agriculture/settlement land was observed at the expense of forestland, woodland, grassland/rangeland, and scrubland/bushland in the Welmel Watershed. Generally, it can be concluded that the Welmel watershed has undergone a significant LULC change in the last 31 years and it is expected to continue in the coming 31 years. Thus, in order to prevent unfavourable effects of these LULC changes, the regional government, the Bale Mountains National Park, and the Woredas in and around the watershed should work together to develop and implement an appropriate plan for safeguarding and managing the current forest and woodlands to preserve natural resources in the watershed.

SUPPLEMENTARY MATERIAL

Supplementary material to this article can be found online at https://www.jwld.pl/files/JWLD-1310-2022-Supplement.pdf.

REFERENCES

Aithal, B.H., Vinay, S. and Ramachandra, T.V. (2013) "Prediction of land use dynamics in the rapidly urbanizing landscape using land change modeler," *Proceedings of International Conference on Advances in Computer Science AET-ACS*, pp. 13–14.

Amini Parsa, V., Yavari, A. and Nejadi, A. (2016) "Spatio-temporal analysis of land use/land cover pattern changes in Arasbaran Biosphere Reserve: Iran", *Modeling Earth Systems and Environment*, 2(4), pp. 1–13. Available at: https://doi.org/10.1007/s40808-016-0227-2.

Andualem, T.G. and Gebremariam, B. (2015) "Impact of land use land cover change on stream flow and sediment yield: A case study of Gilgel Abay watershed, Lake Tana Sub-Basin, Ethiopia," *International Journal of Technology Enhancements and Emerging Engineering Research*, 3, pp. 28–42. Available at: https://issuu.com/ijteee/docs/impact-of-land-use-land-cover-chang/1 (Accessed: May 12, 2022).

Aragaw, H.M., Goel, M.K. and Mishra, S.K. (2021) "Hydrological responses to human-induced land use/land cover changes in the Gidabo River basin, Ethiopia," *Hydrological Sciences Journal*, 66 (4), pp. 640–655. Available at: https://doi.org/10.1080/02626667.2021.1890328.

Araya, Y.H. and Cabral, P. (2010) "Analysis and modeling of urban land cover change in Setúbal and Sesimbra, Portugal," *Remote Sensing*, 2, pp. 1549–1563. Available at: https://doi.org/10.3390/rs2061549.

Aredo, M.R., Hatiye, S.D. and Pingale, S.M. (2021) "Impact of land use/land cover change on stream flow in the Shaya catchment of Ethiopia using the MIKE SHE model," *Arabian Journal of Geosciences*, 14(2), 114. Available at: https://doi.org/10.1007/s12517-021-06447-2.

Ariti, A.T., Vliet van, J. and Verburg, P.H. (2015) "Land-use and land-cover changes in the Central Rift Valley of Ethiopia: Assessment of perception and adaptation by stakeholders', *Applied Geography*, 65, pp. 28–37. Available at: https://doi.org/10.1016/j.apgeog.2015.10.002.

Ayele, G., Hayicho, H. and Alemu, M. (2019) "Land use land cover change detection and deforestation modeling: in Delomena District of Bale Zone, Ethiopia," *Journal of Environmental Protection*, 10(4), pp. 532–561. Available at: https://doi.org/10.4236/JEP.2019.104031.

Behailu, A. (2010) *Land use and land cover analysis and modeling in South Western Ethiopia: The case of selected resettlement Kebeles in GimboWoreda.* MSc Thesis. Addis Ababa: Addis Ababa University. Available at: http://thesisbank.jhia.ac.ke/id/eprint/5121 (Accessed: July 24, 2010).

Behera, M.D. *et al.* (2012) "Modelling and analyzing the watershed dynamics using Cellular Automata (CA)-Markov model – A geo-information-based approach," *Journal of Earth System Science*, 121(4), pp. 1011–1024. Available at: https://doi.org/10.1007/s12040-012-0207-5.

Belward, A.S. and Skøien, J.O. (2015) "Who launched what, when and why; trends in global land-cover observation capacity from civilian earth observation satellites," *ISPRS Journal of Photogrammetry and Remote Sensing*, 103, pp. 115–128. Available at: https://doi.org/10.1016/J.ISPRSJPRS.2014.03.009.

Berihun, M.L. *et al.* (2019) "Hydrological responses to land use/land cover change and climate variability in contrasting agro-ecological environments of the Upper Blue Nile basin, Ethiopia," *Science of the Total Environment*, 689, pp. 347–365. Available at: https://doi.org/10.1016/j.scitotenv.2019.06.338.

Buraka, T., Elias, E. and Lelago, A. (2022) "Analysis and prediction of land-use and land-cover changes and driving forces by using GIS and remote sensing in the Coka watershed, Southern Ethiopia," *Indian Journal of Agricultural Research*, 56(5), pp. 581–587. Available at: https://doi.org/10.18805/IJARe.A-699.

Camara, M. *et*. (2020) "Integrating cellular automata Markov model to simulate future land use change of a tropical basin," *Global Journal of Environmental Science and Management*, 6(3), pp. 403–414. Available at: https://doi.org/10.22034/gjesm.2020.03.09.

Dereje, D. (2010) *Impact of land-use change on reservoir sedimentation (case study of Karadobi).* MSc Thesis. Addis Ababa: Addis Ababa University.

Dibaba, W.T., Demissie, T.A. and Miegel, K. (2020) "Watershed hydrological response to combined land use/land cover and climate change in highland Ethiopia: Finchaa catchment," *Water*, 12(6), 1801. Available at: https://doi.org/10.3390/w12061801.

FAO (2010) "Global forest resources assessment 2010. Main report," *FAO Forestry Paper*, 163. Rome: Food and Agriculture Organization of the United Nations.

Gashaw, T., Bantider, A. and Mahari, A. (2014) "Evaluations of land use/land cover changes and land degradation in Dera District, Ethiopia: GIS and remote sensing-based analysis," *International Journal of Scientific Research in Environmental Sciences*, 2(6), pp. 199–208.

Gashaw, T. *et al.* (2017) "Evaluation and prediction of land use/land cover changes in the Andassa watershed, Blue Nile Basin, Ethiopia," *Environmental Systems Research*, 6(1), 17. Available at: https://doi.org/10.1186/s40068-017-0094-5.

Gashaw, T. *et al.* (2018) "Estimating the impacts of land use/land cover changes on Ecosystem Service Values: The case of the Andassa watershed in the Upper Blue Nile basin of Ethiopia," *Ecosystem Services*, 31, pp. 219–228. Available at: https://doi.org/10.1016/j.ecoser.2018.05.001.

Gebrehiwot, S.G., Taye, A. and Bishop, K. (2010) "Forest cover and stream flow in a headwater of the Blue Nile: Complementing observational data analysis with community perception," *Ambio. A Journal of the Human Environment*, 39(4), pp. 284–294. Available at: https://doi.org/10.1007/s13280-010-0047-y.

Gebremicael, T.G. *et al.* (2013) "Trend analysis of runoff and sediment fluxes in the Upper Blue Nile basin: A combined analysis of statistical tests, physically-based models and land use maps," *Journal of Hydrology*, 482, pp. 57–68. Available at: https://doi.org/10.1016/j.jhydrol.2012.12.023.

Gebreslassie, H. (2014) "Land use-land cover dynamics of Huluka watershed, Central Rift Valley, Ethiopia," *International Soil and Water Conservation Research*, 2(4), pp. 25–33. Available at: https://doi.org/10.1016/S2095-6339(15)30055-1.

Geremew, A.A. (2013) *Assessing the impacts of land use and land cover change on hydrology of watershed: A case study on Gigel-Abbay Watershed, Lake Tana Basin, Ethiopia*. MSc Thesis. Available at: https://run.unl.pt/bitstream/10362/9208/1/TGEO0098.pdf (Accessed: May 10, 2013).

Gidey, E. *et al.* (2017) "Cellular automata and Markov Chain (CA_Markov) model-based predictions of future land use and land cover scenarios (2015–2033) in Raya, northern Ethiopia," *Modeling Earth Systems and Environment*, 3(4), pp. 1245–1262. Available at: https://doi.org/10.1007/s40808-017-0397-6.

Hailemariam, S.N., Soromessa, T. and Teketay, D. (2016) "Land use and land cover change in the bale mountain eco-region of Ethiopia during 1985 to 2015," *Land*, 5(4), 41. Available at: https://doi.org/10.3390/land5040041.

Haregeweyn, N. *et al.* (2015) "Dynamics of land use and land cover and its effects on hydrologic responses: Case study of the Gilgel Tekeze catchment in the highlands of Northern Ethiopia," *Environmental Monitoring and Assessment*, 187(1), pp. 1–14. Available at: https://doi.org/10.1007/s10661-014-4090-1.

Haregeweyn, N. *et al.* (2017) "Comprehensive assessment of soil erosion risk for better land use planning in river basins: Case study of the Upper Blue Nile River," *Science of the Total Environment*, 574, pp. 95–108. Available at: https://doi.org/10.1016/j.scitotenv.2016.09.019.

Hassen, E.E. and Assen, M. (2018) "Land use/cover dynamics and its drivers in Gelda catchment, Lake Tana watershed, Ethiopia," *Environmental Systems Research*, 6(1), 4. Available at: https://doi.org/10.1186/s40068-017-0081-x.

He, C. *et al.* (2019) "Detecting global urban expansion over the last three decades using a fully convolutional network," *Environmental Research Letters*, 14(3), 034008. Available at: https://doi.org/10.1088/1748-9326/aaf936.

Hua, A.K. (2017) "Application of CA-Markov model and land-use/land cover changes in Malacca River watershed, Malaysia," *Applied Ecology and Environmental Research*, 15(4), pp. 605–622. Available at: https://doi.org/10.15666/aeer/1504_605622.

Hyandye, C. and Martz, L.W. (2017) "A Markovian and cellular automata land-use change predictive model of the Usangu catchment," *International Journal of Remote Sensing*, 38(1), pp. 64–81. Available at: https://doi.org/10.1080/01431161.2016.1259675.

Kazak, J.K. (2018) "The use of a decision support system for sustainable urbanization and thermal comfort in adaptation to climate change actions – The case of the Wrocław larger urban zone (Poland)," *Sustainability*, 10(4), 1083. Available at: https://doi.org/10.3390/su10041083.

Keshtkar, H. and Voigt, W. (2016) "A spatiotemporal analysis of landscape change using an integrated Markov Chain and cellular automata models," *Modeling Earth Systems and Environment*, 2(1), 10. Available at: https://doi.org/10.1007/s40808-015-0068-4.

Kumar, K.S. *et al.* (2015) "Prediction of future land use land cover changes of Vijayawada City using remote sensing and GIS," *International Journal of Innovative Research in Advanced Engineering*, 2(3), pp. 91–97.

Kumar, S., Radhakrishnan, N. and Mathew, S. (2014) "Land use change modelling using a Markov model and remote sensing," *Geomatics, Natural Hazards and Risk*, 5(2), pp. 145–156. Available at: https://doi.org/10.1080/19475705.2013.795502.

Lambin, E.F. and Meyfroidt, P. (2011) "Global land use change, economic globalization, and the looming land scarcity," *Proceedings of the National Academy of Sciences*, 108(9), pp. 3465–3472. Available at: https://doi.org/10.1073/pnas.1100480108.

Leta, M.K., Demissie, T.A. and Tränckner, J. (2021) "Hydrological responses of watershed to historical and future land use land cover change dynamics of nashe watershed, Ethiopia," *Water*, 13(17), 2372. Available at: https://doi.org/10.3390/w13172372.

Mango, L.M. (2010) "Modeling the effect of land use and climate change scenarios on the water flux of the upper Mara River flow, Kenya," *FIU Electronic Theses and Dissertations*, 159. Available at: https://doi.org/10.25148/etd.FI10041632.

Mango, L.M. *et al.* (2011) "Land use and climate change impacts on the hydrology of the upper Mara River Basin, Kenya: Results of a modeling study to support better resource management," *Hydrology and Earth System Sciences*, 15(7), pp. 2245–2258. Available at: https://doi.org/10.5194/hess-15-2245-2011.

Matlhodi, B. *et al.* (2019) "Evaluating land use and land cover change in the Gaborone dam catchment, Botswana, from 1984–2015 using GIS and remote sensing," *Sustainability*, 11(19), 5174. Available at: https://doi.org/10.3390/su11195174.

Mengistu, K.T. (2009) *Watershed hydrological responses to changes in land use and land cover, and management practices at Hare watershed, Ethiopia*. PhD Thesis. Siegen: Universität Siegen.

Mezgebu, A. and Workineh, G. (2017) "Changes and drivers of afro-alpine forest ecosystem: Future trajectories and management strategies in Bale eco-region, Ethiopia," *Ecological Processes*, 6(1), 42. Available at: https://doi.org/10.1186/s13717-017-0108-2.

Mishra, V.N. and Rai, P.K. (2016) "A remote sensing aided multi-layer perceptron-Markov Chain analysis for land use and land cover change prediction in Patna district (Bihar), India," *Arabian Journal of Geosciences*, 9(4), 249. Available at: https://doi.org/10.1007/s12517-015-2138-3.

Mishra, V.N., Rai, P.K. and Mohan, K. (2014) "Prediction of land use changes based on land change modeler (LCM) using remote sensing: A case study of Muzaffarpur (Bihar), India," *Journal of the Geographical Institute "Jovan Cvijic", SASA*, 64(1), pp. 111–127. Available at: https://doi.org/10.2298/IJGI1401111M.

MoWR (2007) *Genale Dawa River basin integrated resources development master plan study*, Vo. I-IV (21 volumes). Addis Ababa: Ministry of Water Resources.

Omar, N.Q. *et al.* (2014) "Markov CA, multi regression, and multiple decision making for modeling historical changes in Kirkuk City, Iraq," *Journal of the Indian Society of Remote Sensing*, 42(1),

pp. 165–178. Available at: https://doi.org/10.1007/s12524-013-0311-2.

Rientjes, T.H.M. *et al.* (2011) "Changes in land cover, rainfall and stream flow in Upper Gilgel Abbay catchment, Blue Nile basin – Ethiopia," *Hydrology and Earth System Sciences*, 15(6), pp. 1979–1989. Available at: https://doi.org/10.5194/hess-15-1979-2011.

Saah, D. *et al.* (2019) "Collect Earth: An online tool for systematic reference data collection in land cover and use applications," *Environmental Modelling & Software*, 118, pp. 166–171. Available at: https://doi.org/10.1016/j.envsoft.2019.05.004.

Sang, L. *et al.* (2011) "Simulation of land use spatial pattern of towns and villages based on CA–Markov model," Mathematical and Computer Modelling, 54(3–4), pp. 938–943. Available at: https://doi.org/10.1016/j.mcm.2010.11.019.

Seto, K.C., Güneralp, B. and Hutyra, L.R. (2012) "Global forecasts of urban expansion to 2030 and direct impacts on biodiversity and carbon pools," *Proceedings of the National Academy of Sciences*, 109(40), pp. 16083–16088. Available at: https://doi.org/10.1073/pnas.1211658109.

Shi, H. *et al.* (2012) "RS and GIS-based analysis of landscape pattern changes in urban-rural ecotone: A case study of Daiyue District, Tai'an City, China," *Journal of Landscape Research*, 4(9), pp. 20–23.

Singh, S.K. *et al.* (2018) "Modelling of land use land cover change using earth observation data-sets of Tons River Basin, Madhya Pradesh, India," *Geocarto International*, 33(11), pp. 1202–1222. Available at: https://doi.org/10.1080/10106049.2017.1343390.

SOS Sahel Ethiopia (2010) *Annual accomplishment report for 2009. Submitted to Charities and Societies Agency (CSA)*. Addis Ababa, Ethiopia.

Subedi, P., Subedi, K. and Thapa, B. (2013) "Application of a hybrid cellular automaton–Markov (CA-Markov) model in land-use change prediction: A case study of Saddle Creek drainage basin, Florida," *Applied Ecology and Environmental Sciences*, 1(6), pp. 126–132. Available at: https://doi.org/10.12691/aees-1-6-5.

Tadese, S., Soromessa, T. and Bekele, T. (2021) "Analysis of the current and future prediction of land use/land cover change using remote sensing and the CA-Markov model in Majang Forest Biosphere Reserves of Gambella, southwestern Ethiopia," *The Scientific World Journal*, 2021, 6685045. Available at: https://doi.org/10.1155/2021/6685045.

Taelman, S.E. *et al.* (2016) "Accounting for land use in life cycle assessment: the value of NPP as a proxy indicator to assess land use impacts on ecosystems," *Science of the Total Environment*, 550, pp. 143–156. Available at: https://doi.org/10.1016/j.scitotenv.2016.01.055.

UNDP (2016) *Sustainable urbanization strategy. UNDP support to sustainable, inclusive and resilient cities in developing world*. New York: United Nations Development Programme. Available at: https://www.undp.org/sites/g/files/zskgke326/files/publications/UNDP_Urban-Strategy.pdf (Accessed: December 16, 2016).

Yeshaneh, E. *et al.* (2013) "Identifying land use/cover dynamics in the Koga catchment, Ethiopia, from multi-scale data, and implications for environmental change," *ISPRS International Journal of Geo-Information*, 2(2), pp. 302–323. Available at: https://doi.org/10.3390/ijgi2020302.

Yohannes, H. *et al.* (2020) "Changes in landscape composition and configuration in the Beressa watershed, Blue Nile basin of Ethiopian Highlands: Historical and future exploration," *Heliyon*, 6(9), e04859. Available at: https://doi.org/10.1016/j.heliyon.2020.e04859.

Zhan, J. *et al.* (2014) "Land use change dynamics model compatible with climate models," in X. Deng *et al.* (eds.) *Land use impacts on climate*. Heidelberg: Springer. Available at: https://doi.org/10.1007/978-3-642-54876-5_2.